# A scenario-based stochastic optimization model for charging scheduling of electric vehicles under uncertainties of vehicle availability and charging demand

Wang, Zongfei; Jochem, Patrick; Fichtner, Wolf

**How to cite**

WANG, Zongfei, JOCHEM, Patrick, FICHTNER, Wolf. A scenario-based stochastic optimization model for charging scheduling of electric vehicles under uncertainties of vehicle availability and charging demand. In: Journal of cleaner production, 2020, vol. 254, p. 119886. doi: 10.1016/j.jclepro.2019.119886

This publication URL: https://archive-ouverte.unige.ch/unige:161929

Publication DOI: 10.1016/j.jclepro.2019.119886

Journal Pre-proof

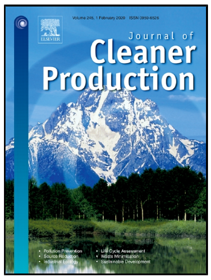


A Scenario-Based Stochastic Optimization Model for Charging Scheduling of Electric Vehicles under Uncertainties of Vehicle Availability and Charging Demand

Zongfei Wang, Patrick Jochem, Wolf Fichtner

| | |
|---|---|
| PII: | S0959-6526(19)34756-0 |
| DOI: | https://doi.org/10.1016/j.jclepro.2019.119886 |
| Reference: | JCLP 119886 |
| To appear in: | *Journal of Cleaner Production* |
| Received Date: | 04 August 2019 |
| Accepted Date: | 25 December 2019 |

Please cite this article as: Zongfei Wang, Patrick Jochem, Wolf Fichtner, A Scenario-Based Stochastic Optimization Model for Charging Scheduling of Electric Vehicles under Uncertainties of Vehicle Availability and Charging Demand, *Journal of Cleaner Production* (2019), https://doi.org/10.1016/j.jclepro.2019.119886

Wordcount: 9345 words

# A Scenario-Based Stochastic Optimization Model for Charging Scheduling of Electric Vehicles under Uncertainties of Vehicle Availability and Charging Demand

Zongfei Wang*, *zongfei.wang@partner.kit.edu*
Patrick Jochem, *patrick.jochem@kit.edu*
Wolf Fichtner, *wolf.fichter@kit.edu*
*Corresponding author

Chair of Energy Economics
Institute for Industrial Production
Karlsruhe Institute of Technology
Hertzstr. 16, 76187 Karlsruhe, Germany

**Abstract**

The integration of electric vehicles (EVs) into the electricity systems comprises both threats and chances. A successful control strategy of EV charging processes is beneficial for both EVs and electricity grid. This paper proposes a scenario-based two-stage stochastic linear programming model for scheduling EV charging processes for different grid requirements in real time using a rolling window approach. The model considers the uncertainties in EV availability (i.e. arrival time and departure time) and electricity demand upon arrival (i.e. initial and target state of charge of the battery). Monte Carlo simulation shows how different input parameters may affect the results. Inhomogeneous Markov Chains are used for EV usage pattern simulation and for scenario generation. For reducing computing time, the amount of scenarios is again reduced by scenario reduction technique. The proposed model is applicable for various grid purposes. We demonstrate the applicability of our model by three example cases: Load flattening (only EV charging load), load leveling (together with conventional household load) and demand response (for wind energy integration or ancillary service).

**Keywords**

Electric vehicles, Smart charging, Uncertainty, Stochastic optimization, Demand response

**Nomenclature**

*Indices/Sets:*

| | |
|---|---|
| $m(EV^i)$ | Electric vehicles (EVs) that are available for charging at period $i$ |
| $t$ | Time intervals |
| $s$ | Time intervals (for estimation of future EV arrivals) |
| $\omega$ | Scenarios |

*Parameters:*

| | |
|---|---|
| $\lambda$ | Penalty factor |
| $Cap$ | Capacity of an EV, [kWh] |
| $e$ | EV charging efficiency, [%] |
| $\Delta t$ | Length of a time interval, [hour] |
| $P^{max}$ | Maximum EV charging power of an EV, [kW] |
| $i$ | Starting period of a rolling window |
| $A_{m,t}$ | Availability of EV $m$ in period $t$, [binary] |
| $SOC_m^{ini}$ | Initial state of charge (SOC) of EV $m$ before charging, [%] |
| $SOC_0^{'}$ | Initial SOC for EVs that are estimated to arrive in future periods, [%] |
| $SOC^{max}$ | Maximum SOC of EV, [%] |
| $SOC_m^{target}$ | SOC target of EV $m$ when charging ends, [%] |
| $SOC_s^{target}$ | SOC target of EV from future period $s$ when charging ends, [%] |
| $\alpha_{s,\omega}$ | Number of EVs that are estimated to arrive in future period $s$ in scenario $\omega$ |
| $W^i$ | Ending period of the rolling window that starts in period $i$ |
| $AA_m$ | Availability of EV $m$ after the rolling window that starts in period $i$, [binary] |
| $D_t^{pref}$ | Preferred total EV charging demand in period $t$, [kW] |
| $\pi_\omega$ | Probability of scenario $\omega$ |

$D_{i-1}$ Total EV charging power in the period before the rolling window which starts in period $i$, [kW]

*Variables (non-negative):*

$Gap_m$ Gap between $SOC_m^{target}$ and SOC of EV $m$ when the rolling windows ends, [%]

$Gap'_{s,\omega}$ Gap between $SOC_s^{target}$ and SOC of EVs from future period $s$ in scenario $\omega$, [%]

$D_{t,(\omega)}$ EV charging demand assumed in period $t$ (in scenario $\omega$), [kW]

$SOC_{m,t}$ SOC of EV $m$ in period $t$, [%]

$SOC'_{s,t,\omega}$ SOC of EVs in period $t$ in scenario $\omega$, [%]

$P_{m,t}$ Charging power of EV $m$ in period $t$, [kW]

$P'_{s,t,\omega}$ Charging power in period $t$ of EVs from period $s$ in scenario $\omega$, [kW]

$D^I_{t,(\omega)}$ Difference between $D^{total}_{t,(\omega)}$ and $D^{pref}_t$ in period $t$ (in scenario $\omega$), [kW]

$D^{II}_{t,\omega}$ Change of $D^I_{t,\omega}$ in two consecutive periods in period $t$ in scenario $\omega$, [kW]

*Notation:*

$\min(\cdot,\cdot)$ Minimum of the two numbers

$\max\{\cdots\}$ Maximum value in the set

## 1. Introduction

With an increasing market share of electric vehicles (EVs), large integration of EVs may bring both challenges and opportunities to the power system (Fischer et al., 2019; Wellers et al., 2016). When EV customers charge EVs without external incentives, they prefer to charge EVs to their desired level as quickly as possible, which is often referred to as uncontrolled charging, or instant charging. By contrast, controlled charging means either EV's charging power is regulated within the given limits or the charging time is scheduled. We do not consider bidirectional charging (so called vehicle-to-grid or V2G) here. With instant charging, EVs will immediately start charging upon arrival with their maximum charging power until their charging targets are completed (Perez et al., 2017; Taljegard et al., 2019; Zhang et al., 2018). This leads to high peak loads, mainly during evening hours, which challenges the electricity grid and may influence the operation of power plants (Schill and Gerbaulet, 2015).

However, due to long idle time, the load shifting potential of EVs is significant and might accordingly be used to alleviate the challenge to the electricity system (Babrowski et al., 2014). The topic of integrating EVs synergistically into the electricity system has gained increasing attention in the literature. Moreover, the promising load shift potential of EVs provides not only the possibility of peak shaving but also the prospect for other applications (J. Hu et al., 2016; Yang et al., 2015). Many literatures focus on the integration of renewable energy with EVs (Goonewardena and Le, 2012; Mehrjerdi and Rakhshani, 2019; Seddig et al., 2017; Yang et al., 2015). Another interesting topic is to maximize the profit of an EV aggregator by participating in the electricity market (Baringo and Sánchez Amaro, 2017; Sarker et al., 2016).

As a foundation of all the promising EV applications above, EV charging behaviors should be scheduled when they are connected to the grid and these behaviors depend on the uncertainties of EV availabilities (i.e. arrival and departure time and the charging demand upon arrival). These uncertainties would deteriorate the practicability of an EV charging scheduling model. Most current literature either assume perfect information about these uncertainties or only consider one of them. Therefore, this paper aims to develop a real-time EV charging scheduling model with a focus on the inevitable uncertainties from EV availability. Moreover, as current studies mostly apply EV's load shifting potential for one specific objective (e.g. load flattening), we structure the model in a flexible way so that it can be easily extensible for different specific applications.

In terms of optimization methods, Sundström and Binding (2012) develop both quadratic and linear programming models which satisfy EV owners' requirements while avoiding distribution grid constraints, and point out the computational challenge of quadratic programming. Both Iversen et al. (2014) and Wu et al. (2016) apply stochastic dynamic programming to minimize the operational cost of a single EV but not an EV fleet. Multi-objective optimization is also applied to balance the tradeoff between conflicting objectives (Ju et al., 2016; Lu et al., 2018), such as demand response and renewable energy integration. When V2G is considered, mixed integer linear programming is often applied because of the binary nature of decision variables for charging or discharging state (Sabillon Antunez et al., 2016).

In this paper, we propose a scenario-based two-stage stochastic linear programming (SLP) model for EV charging scheduling in real time. EV usage patterns are generated by inhomogeneous Markov chains. With regards to real-time scheduling, this myopic (online or local) optimizing environment is considered by a rolling window approach. In the model formulation, future EVs are aggregated by their arrival time so that their uncertainties (i.e. the availabilities and charging demand) are considered by scenario-based stochastic optimization. Representative scenarios are selected by a scenario reduction technique. With Monte Carlo simulation, we further demonstrate the performance of the model with different input parameters (EV usage profiles and their electricity demand). The aggregation of future EVs also keeps the computing time compatible for empirical applications, since we capture their uncertainties in the model but limit the consequential complexities.

The formulation of the model objective is kept slim and as general as possible in order to guarantee its flexible and straightforward application. The model objective is to minimize the distance between the EV charging demand and a pre-defined curve. By simply adjusting this pre-defined curve, we demonstrate the performance of our model using three potential applications. The first application is for load flattening of the charging demand of EV fleets. With the conventional load from households, the second application is for load leveling (peak shaving and valley filling). The last application is related to demand response for wind energy integration and ancillary services in the reserve market.

Our main contributions to the current literature are summarized as follows:

(1) We develop a stochastic optimization model for EV charging scheduling in real time which especially considers the uncertainties from EV availabilities and their demand upon arrival. We also demonstrate the value of using a stochastic model by comparing with a deterministic one.
(2) The objective of the proposed model is formulated in a flexible way and is ready to be implemented for specific applications by only setting different values to one parameter. We extensively present three examples to elaborate the method.
(3) Our problem is applied on empirical field test data represented by usage patterns of dozens of EVs for over six months.

The remainder of the paper is organized as follows. Section 2 gives a short overview of current literature on the EV charging scheduling problem and the current research gap is discussed. Section 3 outlines the formulation of the model. Section 4 explains the setting of the parameters in the model. Section 5 presents three potential applications of the model. Section 6 concludes the paper.

## 2. Related Work

This section gives an overview of current literature focusing on EV charging scheduling problem. The consequential uncertainties are clarified and the research gap is discussed.

### 2.1 Objectives for EV Charging Scheduling

There are two typical ways to schedule EV charging behaviors: the decentralized and the centralized way (Richardson et al., 2012; Sundström and Binding, 2011). The decentralized way means that EVs schedule their own charging behaviors based on information they can receive from outside. Wu et al. (2016) develop a stochastic dynamic programming model to minimize the energy cost of a smart home with EV, battery storage, and photovoltaic array. Iverson et al. (2014) also apply stochastic dynamic programming for charging scheduling of a single EV to minimize the operating cost. A potential drawback of this way is that if multiple EVs receive the same external information (e.g. electricity price) and schedule their charging behaviors under the same strategy, it is likely that their schedules are similar, and this may lead to peak shifting but not peak shaving (Ramchurn, 2012). However, Hu et al. (2016) propose a dynamic pricing mechanism which offers different charging tariffs for EV users depending on their arrival times and the current demand.

The centralized approach means that an entity would schedule charging behaviors for a group of EVs by controlling the charging processes directly or indirectly, e.g. by giving price incentives. This new entity is often referred to as charging service provider, EV aggregator or fleet operator (J. Hu et al., 2016; Sundström and Binding, 2011). Such charging service provider can be the grid operator or a new third-party player that makes a profit by providing demand-side management service. State of charge (SOC), the level of battery charge in percentage, is a key indicator for EV charging scheduling. Together with initial SOC and target SOC, charging service providers need collect EV information (e.g. battery capacity and maximum charging power) and communicate with EVs to schedule optimal charging behaviors. In order to provide a certain kind of service (e.g. reserve) to the grid, an EV charging scheduling model should have a relatively large amount of EVs to schedule.

Charging service providers can schedule charging behavior for EVs. Literally, the charging service is a service provided to an EV to control its charging behavior and to charge the EV in a certain way. In fact, it is a service primarily to the grid or utility because the initial motivation of controlled charging originates from the potential challenge that the grid might face, as discussed in Section 1. Potential cost savings for EV owners guarantee this possibility. With the discussions above, this paper schedules EV charging behaviors in a centralized way. A centralized model may include EVs connected to one location, e.g. one charging infrastructure or one charging station.

**2.2 How Uncertainties of EV are Considered in Modeling**

In this paper, we clarify and analyze two kinds of uncertainties in EV charging scheduling. One uncertainty is EV's availability for charging, which means EV's arrival time to the grid and its departure time. We categorize EVs into two groups: EVs that are currently connected to the grid and EVs that may arrive in the future. For currently connected EVs, the arrival times are apparently known. Regarding the departure time, it is assumed in this paper that with proper financial incentive EV owners will guarantee their departure times upon arrival and send this information to the charging service provider. Please note that this guaranteed departure time can be earlier than the actual departure time but not later. For future EVs, their availabilities remain unknown in this paper. The other uncertainty is the charging demand upon arrival or the SOC of the EV battery, i.e., the initial SOC upon arrival and target SOC at departure. For currently connected EVs, the initial SOC is known and user's target SOC can also be communicated to the charging service provider. For future EVs, their SOC is not known to the system.

Therefore, the uncertainties of EV charging scheduling we consider are not from EVs that are currently connected to the grid, but from EVs that may arrive in future periods, i.e. from their availability and SOC statuses. Although EV charging scheduling models only optimize solutions for currently connected EVs, the arrival of future EVs should also be taken into account. From a systematic aspect, when we schedule the charging behaviors of currently connected EV over a time span, the arrival of future EVs would also have an impact on the total charging demand of the system and the solutions of currently connected EVs in future periods are accordingly affected. The above discussions on EV charging scheduling and its uncertainties provide a framework and contribute to categorizing and analyzing current studies concerning EV charging scheduling.

One way to handle this future EV availability is to only consider the currently-connected EVs into the model and to recalculate the model with updated information whenever new EV arrives. Guo et al. (2018) propose an online linear programming model to decrease the peak of EV charging demand. He et al. (2012) minimize the total charging cost with a quadratic programming model for real-time charging scheduling problem of EVs. Both Guo et al. (2018) and He et al. (2012) compare their optimal solutions between a global (offline) optimum which has perfect information about future EVs and a local (online) optimum which considers only the currently connected EVs. The resulting differences indicate the necessity of considering uncertainty of future EV arrivals for more empirically-related modelling.

The uncertainties from future EV have also received increasing attention by literature. Lu et al. (2018) propose a multi-objective load dispatch model for a microgrid including distributed generations and electric vehicles. The uncertainties from EV usage behavior and charging load are tackled with Monte Carlo simulation which would not apply in real-time EV charging scheduling problem. Heydarian-Forushani et al. (2016) develop a scenario-based stochastic programming model and study the interaction between EV parking lots and wind energy. In this paper, EVs are both aggregated by their arrival time and departure time. Therefore, there is no individual EV in the model and individual charging target is not considered. Instead of using scenarios, Akhavan-Rezai et al. (2018) build and train an artificial neural network to hourly forecast future EV arrivals. However, the uncertainty in future EVs' departure time is not considered. Wu and Sioshansi (2017) develop a two-stage stochastic optimization model for EV charging scheduling at a fast charging station which minimizes the operating cost and avoids overloading the transformer. Their paper models uncertainties in EV arrival time and charging demands upon arrival. However, this paper assumes the same charging duration for all flexible EVs, so the uncertainty in EV departure time is not considered, and the currently connected EVs are in fact modeled in an aggregated way.

In addition to EVs, an energy scheduling model may also incorporate other components (e.g., electricity price, household loads, photovoltaic and wind energy production and stationary battery storage) e.g. Refs. (Le Goff Latimier et al., 2015; Wu et al., 2016; Zhang et al., 2014). In this paper, the parameters of such components will not be considered uncertain.

**2.3 Rolling Window Approach**

As EV charging is persistently scheduled for EVs that arrive, the rolling window approach, or model predictive control, seems to be highly suitable for real-world charging scheduling models. A charging scheduling model optimizes for a fixed time span ($W$ periods in Fig.1). Every time the model iterates, this time span moves forward by one period. The starting period $i$ and the ending period $W^i$ are updated accordingly, as shown in Fig. 1. The set of EVs that are currently available $EV^i$ is also updated, and so are all parameters indexed by $m$. Although the optimal solutions are calculated for $W$ periods, only the solution for the first period (period $i$) will be implemented.

However, few current literatures take rolling window approach into account. Wu and Sioshansi (2017) further apply it to their model with a fixed optimization horizon of 60 minutes while they assume that all EV charging windows are 40 minutes. He et al. (2012) do not fix their optimization horizon (rolling window) when updating charging schedule but only until the last departure time of the currently-connected EVs. Lee et al. (2019) use model predictive control to reschedule EV charging rates when a new EV arrives or the last computed solution exceeds a certain period. Z. Hu et al. (2016) also suggest that the rolling window approach be further applied upon their proposed model for load valley filling by EV charging.

In spite of its necessity, the rolling window approach may bring further challenges to the performance of an EV charging scheduling model, which is rarely mentioned in the current literature. In reality, it is possible that some currently-connected or future EVs might have their charging windows (availabilities) beyond the defined optimization horizon. The first challenge is how to set charging targets for these EVs by the end of the current optimization horizon. For instance in $k^{th}$ iteration of Fig. 1, a future EV may arrive in period $k + W - 1$ but the optimization horizon ends in period $k + W$. It is highly likely that this future EV is still available for charging after period $k + W$. Therefore, a feasible charging targets should be assigned for such EVs. Second, a proposed model may only guarantee the performance of the solution of the current iteration while the true result is a combination of a series of iterations, which might fluctuate (cf. Fig. 6 below). For example, if the objective of a certain EV charging scheduling model is to flatten the total EV charging demand, the optimization solution for $k^{th}$ iteration would be a flat curve. However, if no EV departs at period $k + 1$ and more EVs arrive at period $k + 1$, the optimization solution for $(k + 1)^{th}$ iteration would also be a flat curve, but operating at a higher level. As only the first-period result of every iteration will be implemented, the actual charging demand might fluctuate.

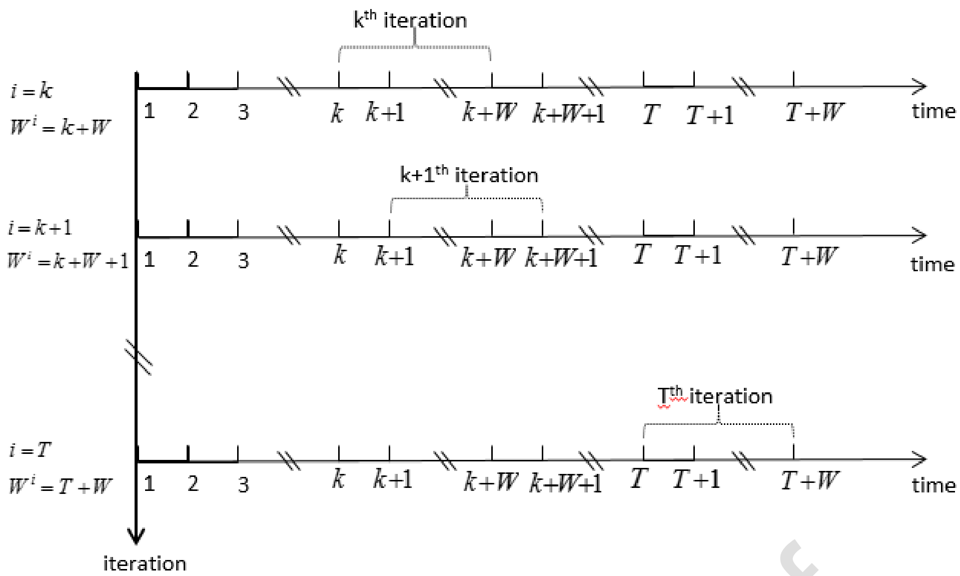

Fig. 1. Illustration of the rolling window approach

### 2.4 Research Gap

With the discussions and the literature review above, the current research gap in EV charging scheduling, where this paper aims to contribute, is mainly on how to consider each EV's uncertainty in the formulation and how to make assumptions in EV parameter settings without oversimplifying them, especially when a model is applied under rolling window approach.

## 3. EV Charging Scheduling Model

We formulate the EV charging scheduling problem as a scenario-based two-stage SLP problem and minimize the distance between the actual EV charging demand and a pre-defined preferred charging demand over a time span. The first stage is only for the current period and determines the charging demand of the EVs that are currently connected to the grid. The second stage is for the rest of the time span and determines the estimated charging demand of the currently connected EVs as well as possible future EVs. For random parameters in the second stage, we use scenarios to represent the possible realizations of the parameters in the second stage.

The model uses the rolling window approach and, hence, only the known EV charging demand in the first stage ($t = i$) for the first 15 minutes are set ultimately (but considering also the estimated future demand). As time moves forward by one period, the optimization horizon also rolls forward by one period and the model recalculates solutions for all following periods ($t > i$) with updated data.

### 3.1 Model Formulation

The formulation of the model is as follows:

Min: $D_i^I + \sum_{\omega}\sum_{t=i+1}^{t=W^i} \pi_\omega \times (|D_{t,\omega}^I| + |D_{t,\omega}^{II}|) + \sum_m Gap_m \times \lambda + \sum_{s,\omega} \pi_\omega \times Gap'_{s,\omega} \times \lambda$ (1)

Subject to:

$D_t = \sum_{m \in EV^i} P_{m,t}$ $\quad t = i$ (2)

$D_{t,\omega} = \sum_{m \in EV^i} P_{m,t} + \sum_{s=i+1}^{t} P'_{s,t,\omega}$ $\quad i+1 \le t \le W^i, \forall\omega$ (3)

$D_t^I = D_t - D_t^{pref}$ $\quad t = i$ (4)

$D_{t,\omega}^I = D_{t,\omega} - D_t^{pref}$ $\quad i+1 \le t \le W^i, \forall\omega$ (5)

$D_{t,\omega}^{II} = D_{t,\omega}^I - D_{t-1,\omega}^I$ $\quad i+1 \le t \le W^i, \forall\omega$ (6)

$SOC_{m,t} \times Cap = SOC_{m,t-1} \times Cap + P_{m,t} \times e \times \Delta t$ $\quad m \in EV^i, i+1 \le t \le W^i$ (7)

$SOC_{m,t} \times Cap = SOC_m^{ini} \times Cap + P_{m,t} \times e \times \Delta t$ $\quad m \in EV^i, t = i$ (8)

$$SOC_{m,t} \leq SOC^{max} \qquad m \in EV^i, i+1 \leq t \leq W^i \qquad (9)$$

$$SOC_{m,t} + Gap_m \geq SOC_m^{target} \times (1 - AA_m) \qquad m \in EV^i, t = W^i \qquad (10)$$

$$P_{m,t} \leq P^{max} \times A_{m,t} \qquad m \in EV^i,\ i+1 \leq t \leq W^i \qquad (11)$$

$$P_{m,t} \leq P^{max} \times (4 - 4 \times SOC_{m,t-1}) \qquad m \in EV^i, i+1 \leq t \leq W^i \qquad (12)$$

$$P_{m,t} \leq P^{max} \times (4 - 4 \times SOC_m^{ini}) \qquad m \in EV^i, t = i \qquad (13)$$

$$SOC'_{s,t,\omega} \times Cap \times \alpha_{s,\omega} = SOC'_{s,t-1,\omega} \times Cap \times \alpha_{s,\omega} + P'_{s,t,\omega} \times e \times \Delta t \qquad i+1 \leq t \leq W^i, i+1 \leq s < t, \forall\omega \qquad (14)$$

$$SOC'_{s,t,\omega} \times Cap \times \alpha_{s,\omega} = SOC'_0 \times Cap \times \alpha_{s,\omega} + P'_{s,t,\omega} \times e \times \Delta t \qquad i+1 \leq t \leq W^i, s = t, \forall\omega \qquad (15)$$

$$SOC'_{s,t,\omega} \leq SOC^{max} \qquad i+1 \leq t \leq W^i, i+1 \leq s \leq t, \forall\omega \qquad (16)$$

$$SOC'_{s,t,\omega} + Gap'_{s,\omega} \geq SOC_s^{target} \qquad t = W^i, s \geq i+1, \forall\omega \qquad (17)$$

$$P'_{s,t,\omega} \leq P^{max} \times \alpha_{s,\omega} \qquad i+1 \leq t \leq W^i, i+1 \leq s \leq t, \forall\omega \qquad (18)$$

As the potential challenge of EV charging is the increase of peak demand within a day, the basic application of our optimization model is peak shaving or load leveling Both Z. Hu et al. (2016) and He et al. (2012) design pricing mechanisms for peak shaving and develop a quadratic programming model to EV charging scheduling. Instead of using electricity price signals as a guidance, this paper proposes to use a preferred total charging demand curve. Objective (1) minimizes the distance between the EV charging curve and this preferred curve and makes sure the distance over a time span could be equally distributed if possible. With Objective (1), the actual total charging demand would try to follow this pre-defined preferred curve. The curve makes the model extensible since the true model task depends on the value of this preferred curve. In (1), $D_i^I$ is the objective function of the first stage, namely the distance between the EV charging demand and the preferred demand only for the current period ($t = i$). $\sum_{\omega}\sum_{t=i+1}^{t=W^i}\pi_\omega \times (|D_{t,\omega}^I| + |D_{t,\omega}^{II}|)$ is the objective function of the second stage, namely the distance for the rest of the time span ($t \in \{i+1,\ldots,W^i\}$). As we use scenarios to represent the uncertain parameters in the future, variables in the second stage are scenario-dependent (indexed by $\omega$) and the objective function of the second stage is a weight average of different scenarios. $\sum_m Gap_m \times \lambda$ and $\sum_{s,\omega}\pi_\omega \times Gap'_{s,\omega} \times \lambda$ are relaxation terms to guarantee that the model will not be infeasible in case EV users' charging target cannot be satisfied. The penalty factor λ here is set to be a very high positive value ($10^6$ in our case). As a result, to meet users' request is prior to following the preferred curve so that the high penalty could be avoided.

Constraints (2)-(6) define the variables in Objective (1). The total EV charging demand $D_i$ and $D_{t,\omega}$ are defined in (2) and (3). Unlike $D_i$, second-stage variable $D_{t,\omega}$ also considers demand from EVs that might arrive in future periods. There are three indices for the charging power of future-connected EVs $P'_{s,t,\omega}$. The first index $s$ points out the future periods when these EVs are estimated to arrive. The second index $t$ stands for the period of a charging behavior. The third index $\omega$ indicates scenarios, as estimations for the number of EV arrivals in the future may vary among scenarios. According to the definition of $P'_{s,t,\omega}$, its charging time $t$ cannot be earlier than the arrival time $s$ (one EV can only be charged upon arrival). For instance, $P'_{2,4,8}$ means that the charging power in period 4 for the EVs that are estimated to arrive in period 2 by scenario 8. By comparison, $P'_{4,2,8}$ means one EV is charged before its arrival time, which is not feasible. In (4), $D_t^I$ and $D_{t,\omega}^I$ are the difference between total charging demand $D_t$ and preferred charging demand $D_t^{pref}$ for the starting period $i$. Similar to $D_t^I$ , $D_{t,\omega}^I$ in (5) is the difference between total charging demand $D_{t,\omega}$ and preferred charging demand $D_t^{pref}$ for the following periods. In (6), $D_{t,\omega}^{II}$ is the change of this difference. $Gap_m$and $Gap'_{s,\omega}$in (1) serve as a relaxation for the model in case it fails to meet the charging target set by a certain user when the charging service ends.

(7) - (13) are for EVs that are currently connected to the grid. (7) - (10) are constraints for EV SOC. (7) and (8) are for SOC in two consecutive periods. (9) guarantees that the SOC will not exceed the maximum value. (10) is to make sure that the SOC target set by the user can be satisfied at the end of the current rolling horizon. Two exceptions are considered in (10). First, $Gap_m$ guarantees that if the

final SOC of an EV is still lower than the SOC target set by the user, the model will not be infeasible. The penalty $\lambda$ is set to be a very high value so that meeting users' request has priority over following preferred charging demands. Second, $AA_m^i$ in (10) is a binary parameter and is equal to 1 when the availability of an EV is beyond the current rolling window horizon. By giving more charging flexibility to EVs that have longer available periods, $AA_m^i$ avoids long periods with high SOC and protects battery lifetime (Lunz et al., 2012). (11) limits the charging power of the EVs. $A_{m,t}$ is the availability of EVs that are currently connected to the grid. The departure times of these EVs are assumed to be known in advance, as explained in Section 2.2. As assumed in Kaschub et al. (2013), EV's maximum charging power will decrease as SOC increases. We also model this maximum charging power decrease in a linearized way. (12) and (13) assume that the maximum charging power will start to decrease linearly when SOC is over 75% and will drop to zero at full SOC.

Constraints (14) - (18) are for EVs that are estimated to arrive in future periods, and are similar to constraints (7) - (11). However, EVs that are estimated to arrive in the same future period are taken as one "aggregated" EV in the model. The number of EVs that arrive in one same future period is a random parameter and we formulate the stochastic problem in a scenario-based way, which means this random parameter is replaced by its weighted scenarios (possible realizations). Such replacement turns a stochastic model into a deterministic one (Seddig et al., 2019; Wu and Sioshansi, 2017). Parameter $\alpha_{s,\omega}$ estimates the number of EVs that may arrive in future periods in different scenarios. The capacity and maximum charging power of these aggregated EV depend on the number of EVs aggregated. With this aggregation, the model does not need to individually consider the uncertainties in departure time and SOC of future EVs. Constraint (14) and (15) are for the SOC of this aggregated EV in two consecutive periods. (16) guarantees that SOC of the aggregated EV will not exceed maximum value. Similar to (10), (17) also sets a charging target for future EVs and considers the uncertainty of future EV departure time. For these aggregated EVs, the charging target $SOC_s^{target}$ by the end of the optimization horizon will be set to be proper values, which will be further discussed in Section 4.2. Linearization of maximum charging power is not applied to these aggregated EVs. (18) limits the charging power of the aggregated EV.

## 4. Parameter Setting

### 4.1 Temporal Setting

With the rolling window approach, newly-arrived EVs can be integrated into the model and the set of connected EVs is always updated. The model optimizes charging scheduling for the next 24 hours and the time resolution is 15 minutes. The setting of 24-hour rolling horizon is because the total charging demand within 24 hours is similar between different rolling windows, although the EV charging demand can be shifted to some extent. The model runs every 15 minutes with updated parameters, hence only the here-and-now solution for the first stage will be actually implemented.

### 4.2 EV setting

#### 4.2.1 EV Usage Pattern

The original EV usage data employed in this paper is from iZEUS (2012), the intelligent Zero Emission Urban System project which aims to enhance research, development, and practical demonstration in the fields of smart traffic and smart grid. From this project, usage patterns of 28 EVs are recorded for six months by minute. The usage data are recorded in three states: driving, parking only and charging. With this data set and inhomogeneous Markov chains (Iversen et al., 2017; Widén et al., 2009), this paper generates EV availability patterns and scenarios for future EV arrivals.

In a nutshell, there are two steps to follow in order to generate EV usage data from inhomogeneous Markov chains. The first step is to obtain the transition matrix for each EV, as shown in (19).

$$M(t) = \begin{bmatrix} p_{11}(t) & p_{12}(t) & p_{13}(t) \\ p_{21}(t) & p_{22}(t) & p_{23}(t) \\ p_{31}(t) & p_{32}(t) & p_{33}(t) \end{bmatrix} \qquad p_{ab}(t) = P(X_{t+1} = b | X_t = a) \qquad (19)$$

In (19), $X_t$ denotes the state of an EV in time $t$. $p_{ab}(t)$ is the transition probability and it denotes the probability of EV to change from state $a$ to state $b$ in time $t$. We use inhomogeneous Markov chains because this transition probability is time-variant within a day. For example, EVs are more likely to remain parked at night than in the day-time. $p_{ab}(t)$ can be estimated from statistical data (original EV trip data in this paper). For example, an EV has two states (0 for parking and 1 for driving) and ($X_t$,$X_{t+1}$ ) denotes EV's state in two consecutive periods. According to original trip data, we have ten samples of ($X_t$,$X_{t+1}$), which are (0,0), (0,1), (0,1), (0,1), (1,0), (1,1), (1,1), (1,1), (1,1) and (1,1). Then we have

$$M(t) = \begin{bmatrix} p_{00}(t) & p_{01}(t) \\ p_{10}(t) & p_{11}(t) \end{bmatrix} = \begin{bmatrix} 1/4 & 3/4 \\ 1/6 & 5/6 \end{bmatrix} \qquad p_{ab}(t) = P(X_{t+1} = b | X_t = a) \quad \text{(19a)}$$

The second step is to generate simulated data by using $M(t)$ and a random number, which is uniformly distributed between 0 and 1. $X_1$, the state at the starting period, can be assumed to be zero. To get the value of $X_2$, we compare $M(1)$ with a random sampling of this random number, say 0.2. If we suppose $M(1)$ is equal to $M(t)$ in (19a), this 0.2 is less than 0.25 and $X_2$ is equal to 0. In such a way, we could generate a time series of EV usage pattern.

We assume that when an EV is not in the driving state, it is available for charging. With this assumption, we convert $X_t$ into each $A_{m,t}$ (a binary parameter in the proposed model). Only availability periods longer than 3 hours are considered for controlled charging, because shorter availability periods are more suitable for instant charging. As a relatively large amount of EVs are necessary for centralized scheduling, this paper generates four availability patterns with each of the 28 transition matrices from inhomogeneous Markov chains so that there are 112 EVs in the model for $A_{m,t}$.

An EV has load shifting potential only when its parking duration is beyond its minimum charging time. A longer extra parking time means a greater load shifting potential, which could also have an impact on the performance of a model. With extra parking time, charging behaviors can be postponed or shifted (Babrowski et al., 2014). Otherwise, instant charging would be the only option. Therefore, we present the simulation data of $A_{m,t}$ (EV availability). In order to present the uncertainty of EV usage patterns, we compare $M(t)$ with repeated random sampling of the random number uniformly distributed between 0 and 1. With 500 runs of Monte Carlo simulation, Fig.2 shows the proportions of EVs' parking events with different durations in the total number of parking events. Fig. 3 shows the number of parked EVs within a day. The curve presents the median and the shaded area is for data between 25% and 75% quantile.

As shown in Fig. 2, on average, about 60% of the parking events we consider have availability durations of less than 12 hours. Schäuble et al. (2017) have similar findings concerning the distribution of charging availability durations. Please note that we only consider EVs with availability periods longer than three hours, as discussed in Section 4.2. Based on the EV settings in Section 4.2.2, it takes about five hours to fully charge an empty EV with maximum charging power in our model. If an EV would like to have a 50% SOC increase within three hours, this leaves almost no potential for load shifting. Even under a controlled charging strategy, its EV charging curve would still behave like one under instant charging strategy. Therefore, due to the EV settings of the paper, we only consider EVs parking more than three hours as they have relatively sufficient potential for load shifting. In Fig. 3, most EV are parked before 6 a.m. and then this parking number decreases in the daytime, which is similar to the findings of Schäuble et al. (2016) and Brady and O'Mahony (2016).

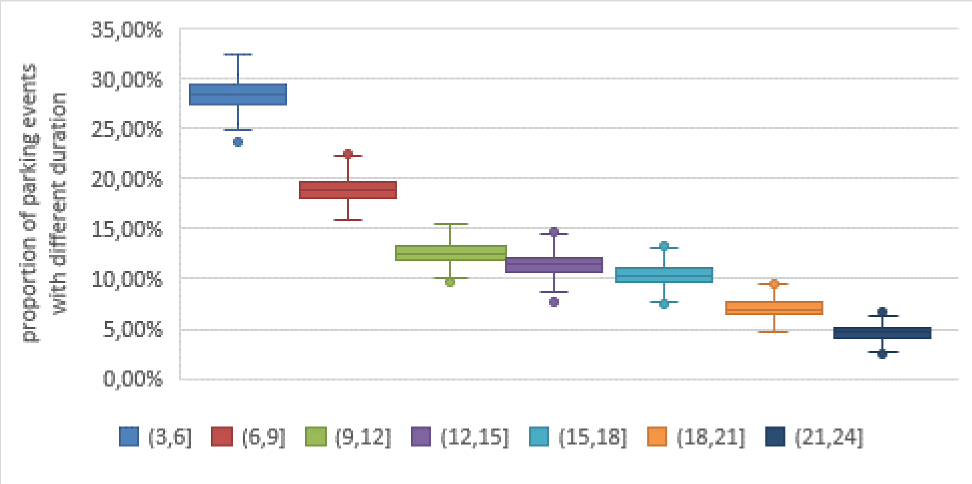


Fig. 2. Box plots of EV parking durations (in blocks of three hours)

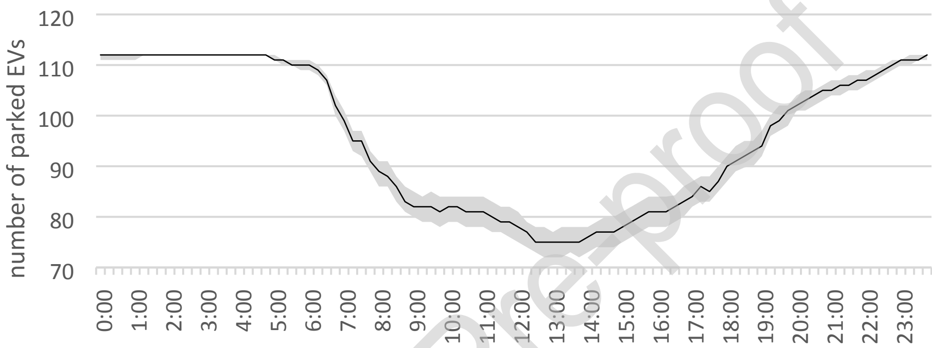


Fig. 3. Distribution of parked EV quantity in every 15 minutes (with median – curve; 25% & 75% quantile - shade)

In order to approximate the uncertainty of random parameter $\alpha_{s,\omega}$, a large set (500) of scenarios is generated with inhomogeneous Markov chains mentioned above. As such a large scenario set would also bring computational challenge to the model, scenario reduction technique is then applied to reduce the number of scenarios used in the model. The commonly used scenario reduction methods are forward selection methods, backward reduction methods and their variants. Both forward selection and backward reduction methods run in an iterative fashion. For one iteration, forward selection methods select one representative scenario out of the original set while backward reduction methods exclude one scenario which could be represented by others. As we plan to pick 10 (a small number of) scenarios out of 500, forward selection takes fewer iterations to solve and outperforms backward reduction in terms of computational time (Wang, 2010). We apply the fast forward selection method (Feng and Ryan, 2013; Heitsch and Römisch, 2003), which is briefly reviewed as follows. The Euclidean distance of each two scenarios is first calculated and one scenario which is closest to the other scenarios can be selected. Then the second scenario can be selected which is closest to the remaining scenarios. The process iterates until the method selects a subset of the original scenario set which includes 10 scenarios and has the shortest distance to the remaining scenarios. A smaller set of scenarios are selected to represent the possible realizations and guarantee low computation time. Unselected scenarios will then add their own probabilities to one of selected ones which has the shortest distance to them.

Fig. 4 presents the distribution of EV arrival quantity and its variation throughout a day and shows the randomness of the stochastic parameter $\alpha_{s,\omega}$. The curve presents the median and the shaded area is for data between 25% and 75% quantile. It can be seen that most arrivals happen after 6 a.m. and peak in the evening hours.

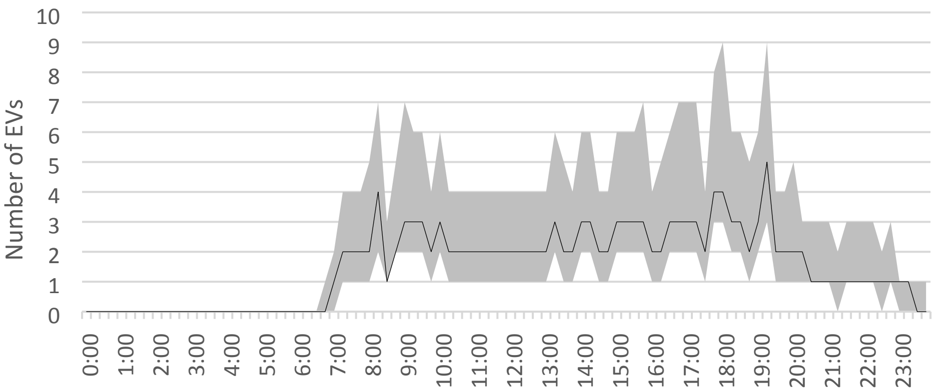


Fig. 4. Distribution of EV arrival quantity in every 15 minutes
(with median – curve; 25% & 75% quantile - shade)

### 4.2.2 EV Model Specification

In the field test of iZEUS (2012), Daimler electric Smart is used for several months generating comprehensive driving and charging patterns. In this paper, the corresponding EV specification in the parameter settings, as listed in Table 1, are considered for the following calculations.

Table 1. EV specification settings

| *Parameter* | *Setting* | *Parameter* | *Setting* |
|---|---|---|---|
| $Cap$ | 17.6 kWh | $e$ | 90% |
| $P^{max}$ | 5 kW | $SOC_m^{ini}$ | $U$(15%,75%) |
| $SOC_0^{'}$ | 45% | $SOC^{max}$ | 100% |

The rationale of Table 1 is to follow the specification of Daimler electric Smart (the car model used in iZEUS). The battery capacity of Daimler electric Smart is 17.6 kWh. 90% is a reasonable assumption for EV charging efficiency. The maximum charging power $P^{max}$ at a standard charging point is usually between 2.5 kW to 7 kW. We assume that the initial battery level $SOC_m^{ini}$ is between 15% and 75 % so that the average value is 45%. In equation (20), we set the target SOC to be 90 % if possible. Therefore, this setting would meet the daily energy consumption of one EV, which is about 8 kWh.

The setting of $SOC_m^{target}$ considers the availability parking duration $T_m$ (in 15 minutes) of each EV and its initial SOC. As in (20), $SOC_m^{target}$ is set to be an appropriate value and is below 90% so that the SOC target can be satisfied within the charging period, and the load shifting potential is also guaranteed. With maximum charging power, the SOC increase of one EV in our model in one period (15 minutes) is about 6%. For flexibility of charging scheduling, we assume a 3% SOC increase per period (half of maximum SOC increase). Since future arrivals of EVs are aggregated, the notion of departure time does not apply to this aggregated EV. The model only needs to assign a proper charging task $SOC_s^{target}$ by the end of a rolling horizon, as is explained in (21). Please note that although (20) and (21) look similar in form, the meanings behind $SOC_m^{target}$ and $SOC_s^{target}$ are different. $SOC_m^{target}$ is the real charging target for the currently connected EVs while $SOC_s^{target}$ assigns charging tasks for the aggregated future EVs and is only an estimation for the future.

$$SOC_m^{target} = \min\,(SOC_m^{initial} + T_m \times 0.03,\, 0.9) \qquad \forall m \qquad (20)$$

$$SOC_s^{target} = \min\,(SOC_0^{'} + (W^i - s) \times 0.03,\, 0.9) \qquad \forall s \qquad (21)$$

## 5. Results and Discussions

In this section, we will illustrate the proposed model with three potential applications. ***Application I*** is to flatten the total charging demand of EVs. With ***Application I***, we compare the performance of our model with that of a deterministic one. ***Application II*** is for peak shaving and valley filling (together with conventional load from households). ***Application III*** contributes to wind energy integration and ancillary services in the reserve market. We also validate the choice of the stochastic model instead of a deterministic one. The formulated model is a two-stage SLP model and includes 260,981 variables and 549,470 constraints. The model is implemented in GAMS with CPLEX solver installed in a personal laptop with Intel Core i5-7200U processor and 8 GB RAM. As the model runs iteratively in a rolling window fashion, it takes about 15 seconds to solve one iteration.

### 5.1 *Application I:* Flattening EV Charging Demand

In order to give a quantitative example of the load shifting potential of EVs, *Application I* is to flatten the EV charging demand, which decreases the peak demand of EV charging and increases the workload of the electricity grid without an additional investment in the new grid hardware, e.g. EV parking lots (Jochem et al., 2016; Lee et al., 2019). To achieve this goal, the preferred demand curve $D_t^{pref}$ is defined in (22). With this, the charging demand curve aims to be as flat and as low as possible. For comparison, we also simulate a charging demand curve for instant charging with the same EV usage data. Our proposed model runs for a two-day time span and results are shown in Fig. 5.

$$D_t^{pref} = 0 \qquad \forall t \tag{22}$$

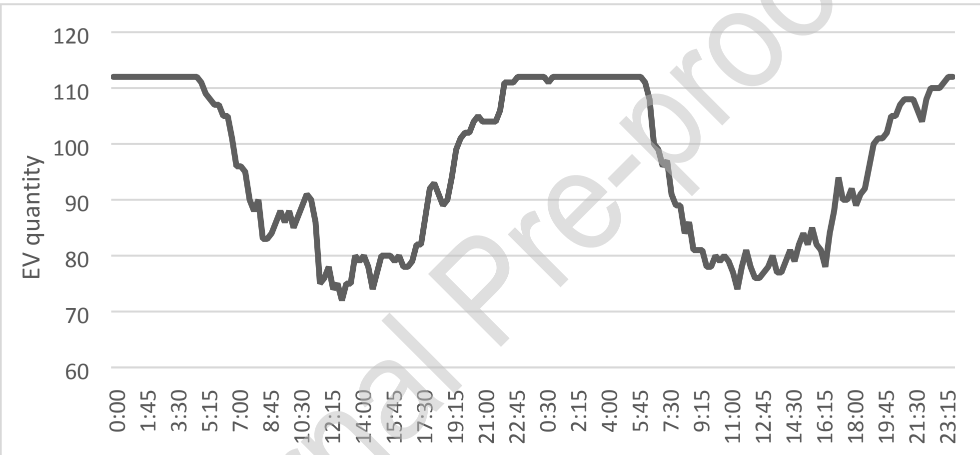


Fig. 5(a). Number of parked EVs

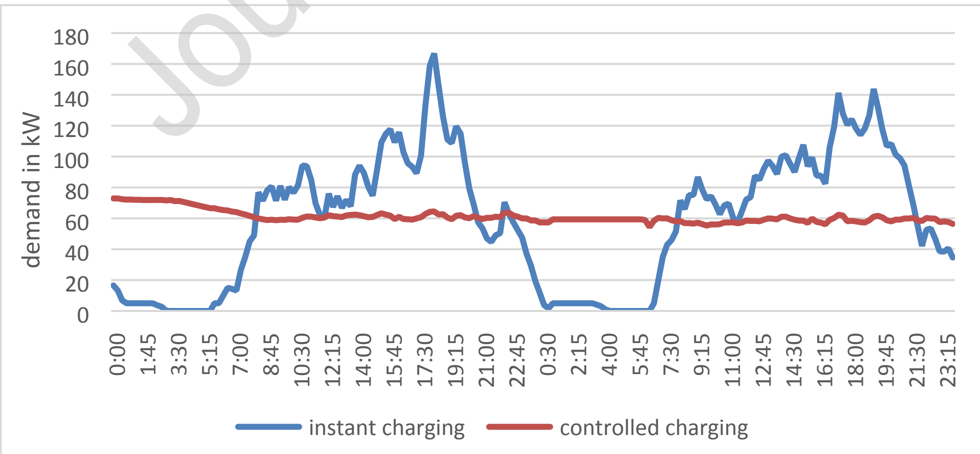


Fig. 5(b). EV charging demand of instant and controlled charging strategy

As discussed in Section 4.2, we assume that all parked EVs have charging requests and are available for charging (connected to the grid). In Fig. 5(a), the number of EVs connected to the grid decreases during daytime. In Fig. 5(b), the instant charging curve is simulated under the assumption that EVs charge upon arrival with maximum charging power until they reach their charging targets. The controlled charging curve is the optimization results of the proposed model where EVs' charging time can be scheduled within their parking time and their charging power can be regulated. The instant charging demand of these EVs peaks significantly in early evening hours and drops to a low level at night time. This simulated result of instant charging demand shows characteristics similar to those found by Schäuble et al. (2017). There is some synergy effect between the instant charging demand and the number of EV arrivals (Fig. 4), which is in line with the definition of instant charging. The instant charging demand depends more on the number of EV arrivals and less on the number of parked EVs. In controlled charging, EV charging demand is flattened and distributed throughout the entire day. The peak demand of instant charging strategy is 167 kW while the peak demand of controlled charging strategy is 73 kW. A potentially applicable situation of this example could be a parking garage or a charging station which might otherwise need to increase its capacity.

**5.2 Comparison of Stochastic and Deterministic Models**

The number of future EV arrivals is the main uncertain parameter in EV scheduling. The proposed model in Section 3 is formulated as a scenario-based stochastic problem for this uncertain parameter ($\alpha_{s,\omega}$). The value of the proposed stochastic model is compared with a deterministic model in which the number of future EV arrivals is estimated with the mean value of each period (cf. Fig. 4). As a benchmark, the solution of a *perfect* model is also presented where we use the real arrival quantity of each future period as an estimation. Please note that all other parameter settings remain the same for all three models. The *perfect* model here is not a perfect foresight model.

To illustrate the performance of the three models, we present their solutions under two new EV usage profiles with ***Application I***, as shown in Fig. 6. In both Fig. 6(a) and Fig. 6(b), the perfect solution is not perfectly flat as other uncertainties still remain ($SOC_0^{'}$ and $SOC_s^{target}$) and the rolling window approach is applied. In spite of that, the perfect solution can serve as a benchmark for the other two solutions. In terms of curve fitting, we introduce two indicators to check whether the stochastic model gives a better fit (closer to the perfect model solution), namely mean absolute error (MAE) and root mean square error (RMSE). For a solution of $n$ periods, $e_j$ is the error for each period ($e_j$, $j = 1,2,\ldots n$). MAE and RMSE are calculated as

$$MAE = \frac{1}{n}\sum_{j=1}^{n} e_j \tag{23}$$

$$RMSE = \sqrt{\frac{1}{n}\sum_{j=1}^{n} e_j^2} \tag{24}$$

With the definitions in (23) and (24), RMSE gives more weight to larger errors while MAE is unbiased. Table 2 shows the comparison results of Fig. 6. The two indicators may or may not draw the same conclusion under different EV usage profiles.

With Monte Carlo simulation, average errors are calculated for 100 random EV usage profiles.. Please note that one random EV usage profile here consists of 112 EV usage behaviors for two days as input data. Furthermore, we present the maximum deviation of a single period and the top 1‰ deviations in Table 3. The overall performance of the two models (stochastic and deterministic) can therefore be presented by various indicators and under a large size of different input data. With the favorable results shown in bold type, the stochastic model is found to give a better curve fitting in terms of avoiding larger deviations (errors). One example of a large deviation is Fig. 6(b) which has a significant load drop around 7:30 a.m. on the first day. However, the stochastic model outperforms the deterministic one under such extreme case.

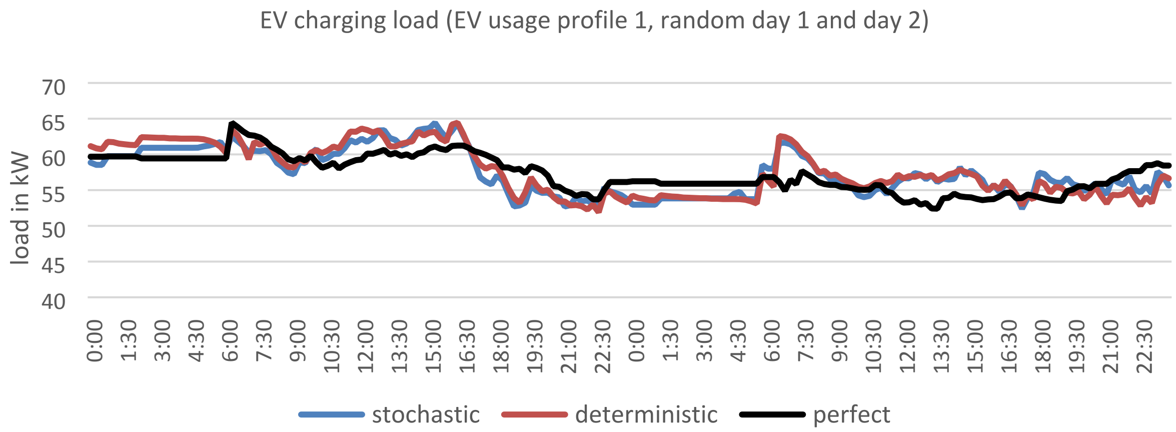


Fig. 6(a). Flattened EV charging load under EV usage profile 1

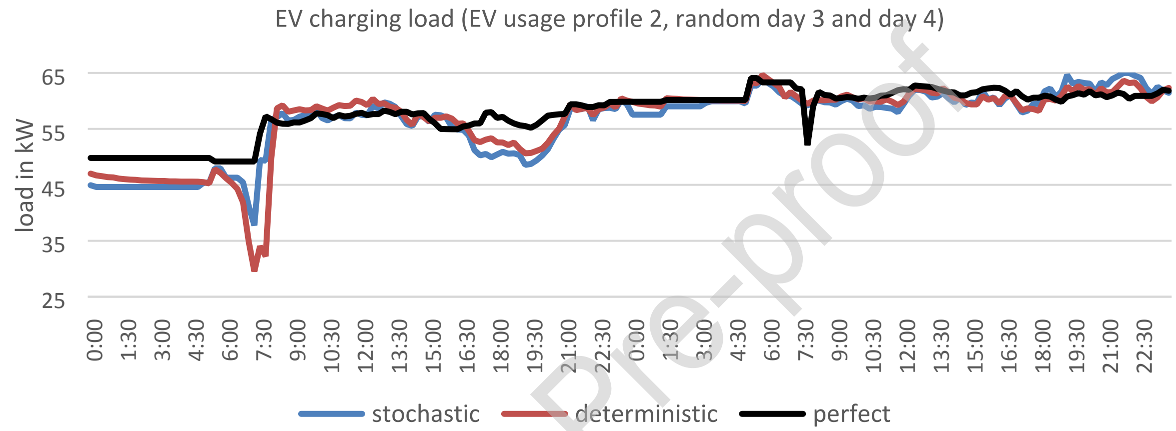


Fig. 6(b). Flattened EV charging load under EV usage profile 2

Table 2. MAE and RMSE under two EV usage profiles of Fig. 6 (kW)

| | MAE | | RMSE | |
|---|---|---|---|---|
| | Stochastic | Deterministic | Stochastic | Deterministic |
| Fig. 6(a) | 1.9491 | 2.1062 | 2.2968 | 2.4377 |
| Fig. 6(b) | 2.3448 | 2.1665 | 3.1476 | 3.7510 |

Table 3. Different criteria for stochastic and deterministic model comparison (kW)

| | Stochastic | Deterministic |
|---|---|---|
| Average MAE | 2.0731 | **2.0223** |
| Average RMSE | **2.6001** | 2.7679 |
| Maximum deviation | **19.2003** | 36.6387 |
| Deviation of top 1‰ | ≥ **11.3074** | ≥ 20.2641 |

### 5.3 *Application II*: Peak Shaving and Valley Filling

More applications of EV charging scheduling are related to the interaction of the latter with other elements in the power systems, e.g., original load, renewable energy and stationary battery storage. According to Sundström and Binding (2012) and Liu (2012), instant charging demand increases significantly during evening hours. This has a negative impact on the electricity system.

*Application II* of the proposed model is to shift EV charging demand for peak shaving and valley filling from conventional load $Base_t$, which refers to the total household load of 112 families. Together with this conventional load, *Application II* shifts more EV charging load to off-peak hours and limits the increase in peak load. The preferred load curve is defined in (25). With Monte Carlo simulation, we present how different input parameters (EV usage patterns and SOC status) may affect the results. Fig. 7 presents 10 Monte Carlo simulation runs of the model with different EV arrival parameters for three days, i.e. EV availability ($A_{m,t}$, $AA_m$) from inhomogeneous Markov chains and SOC status ($SOC_m^{ini}$, $SOC_m^{target}$).

$$D_t^{pref} = max\,\{Base_t \,|\, i+1 \leq t \leq W^i\} - Base_t \qquad \forall t \qquad (25)$$

Fig. 7(a) shows how EV charging load follows the preferred curve under 10 different EV parameters. Because of the charging target set by EV users, the EV charging load may not perfectly reach the value of the preferred curve but is able to follow the shape of the preferred curve under uncertainties. In Fig. 7(b), the black curve is the conventional load $Base_t$. The 10 colored curves above are 10 potential total demand curves out of 10 different EV arrival parameters. The area between each of the 10 colored curves and the base-load black curve is the EV charging load (cf. Fig. 7(a)). As can be seen, EV charging behaviors are more scheduled to off-peak hours in order to avoid higher peak load. The model also manages to cover the variation of the base load without further increasing the peak load. The difference between the 10 total load curves (10 color curves in Fig. 7) derives from the 10 Monte Carlo simulation runs of EV arrival parameters. This result serves as an example to show how the results would perform on different days. Morais et al. (2014) show similar results but EV uncertainties are not considered.

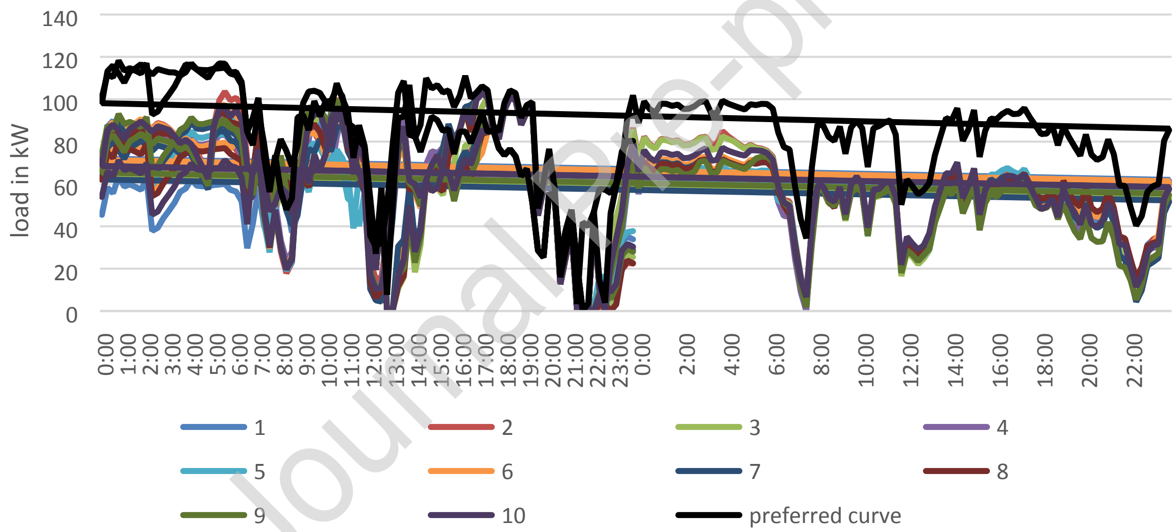


Fig.7(a). EV charging load for peak shaving and valley filling under 10 Monte Carlo simulation runs (charging load - in color; preferred curve - black)

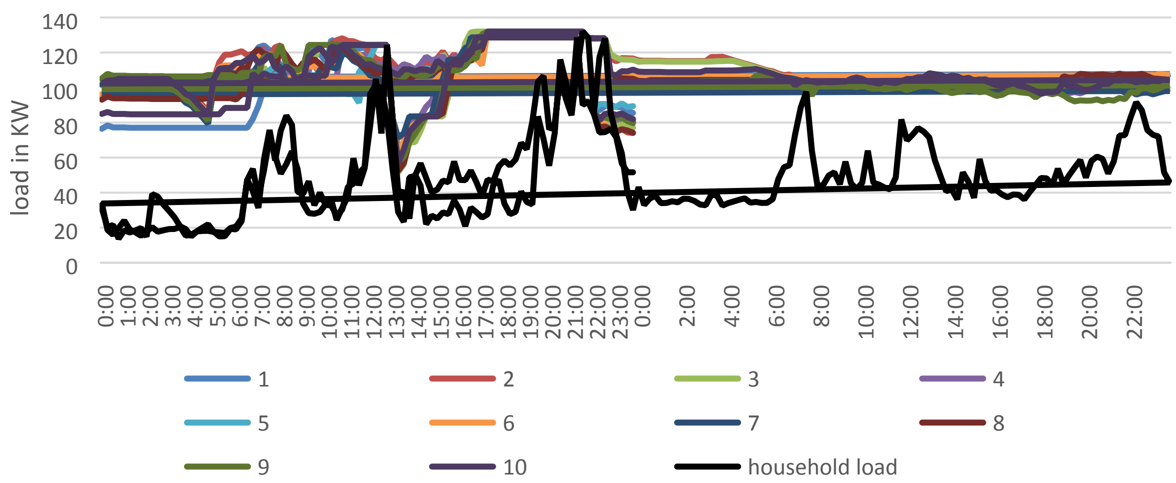


Fig.7(b). Total load for peak-shaving and valley-filling under 10 Monte Carlo simulation runs (total load - in color; household load - black)

**5.4 *Application III*: Demand Response for Wind Energy Integration and Control Reserve Market**

A significant amount of wind energy has been curtailed in the past few years (Schermeyer et al., 2018) and recent literature also considers utilizing EVs for the integration of renewable energy (Schuller et al., 2015). With great temporal flexibility, EVs can be used to reduce the curtailment of wind and solar energy, which is *Application III* of our model.

In the case of potential wind energy curtailment, EV charging demand can adjust accordingly for the utilization of renewable energy. To achieve this goal, the preferred demand curve $D_t^{pref}$ is again set to zero (cf. constraint (22)). Additionally, constraint (26) will be added to the proposed model. When a new rolling window starts, constraint (26) forces the total charging demand $D_{t,\omega}$ in the next few periods to be higher or lower than the previous charging demand $D_{i-1}$ by a certain amount $R$. Scalar $q$ determines the duration of the decrease periods. Exemplary results are shown in Fig. 8.

$$D_{t,\omega} = D_{i-1} + R \qquad i \le t \le i+q, i \ge 2, \forall\omega \tag{26}$$

In Fig. 8(a), a demand increase $R$ of 40 kW for two hours from 7:45 to 9:45 of the first day is requested. For comparison, the reference charging demand (without $R$ request) is also given. As extra EV charging demand is scheduled, EV charging demand after 10 a.m. is lower than the one in the reference case as a compensation. This compensation effect is because the total EV demand within a time frame is fixed to some extent. Our proposed model distributes this compensation smoothly in the following periods and minimizes this side effect. Fig. 8(b) shows a mirrored example of Fig. 8(a) on the demand side, where $R$ is set to be -40 kW between 7:45 and 9:45. When power import is needed because of wind energy curtailment, this problem can be temporarily solved by postponing EV charging, which provides an option to avoid high redispatch cost.

In Fig. 8(c), we further set $R$ to be -50 kW between 7:45 and 10:45 to examine the impact of this application on EVs' final SOC. We find that all EVs' target SOC are completed in the reference case of Fig. 8 while eight charging tasks are not completed in the decrease case of Fig. 8(c). We compare the results of final SOC at departure of these two cases and present our findings in Fig. 9. We illustrate the charging availabilities of the eight tasks with grey bars and the decrease periods with blue shades (from 7:45 to 10:45 of the 1st day). As shown in Fig. 9, these eight charging tasks have relatively shorter availability periods (about 4 hours) and the majority of their availability periods are in the decrease period (3 hours, between 7:45 and 10:45). Because of this overlapping, these charging tasks have limited load shifting potentials beyond the decrease periods. In order to respond to the mandatory demand decrease, these eight charging tasks greatly reduce their charging power between 7:45 and 10:45. As their departure time is too early to outbalance this request, their charging tasks become incomplete.

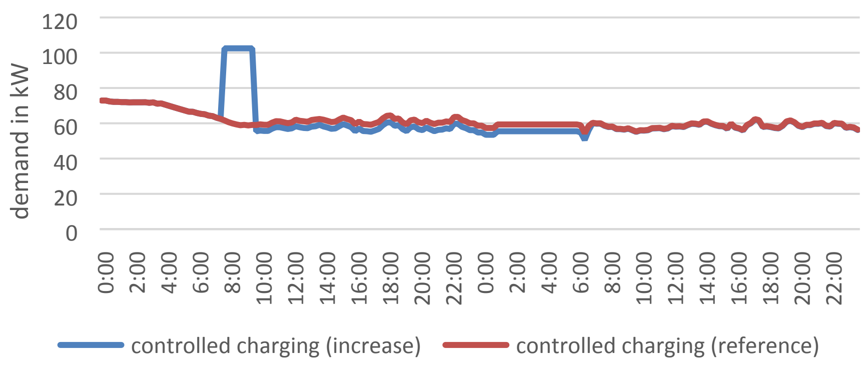


(a) $R = 40\ kW$, between 7:45 and 9:45 of the first day

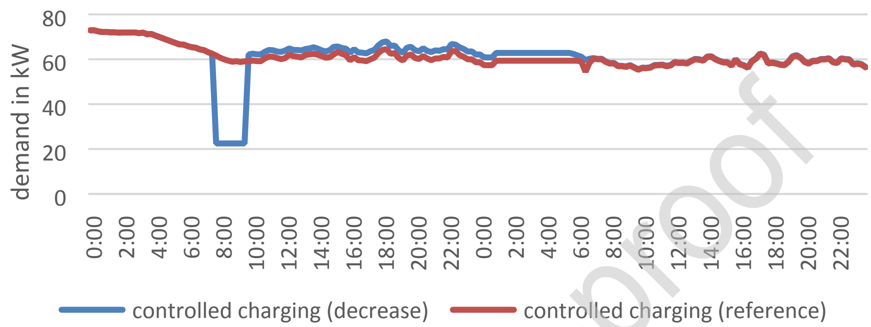


(b) $R = -40\ kW$, between 7:45 and 9:45 of the first day

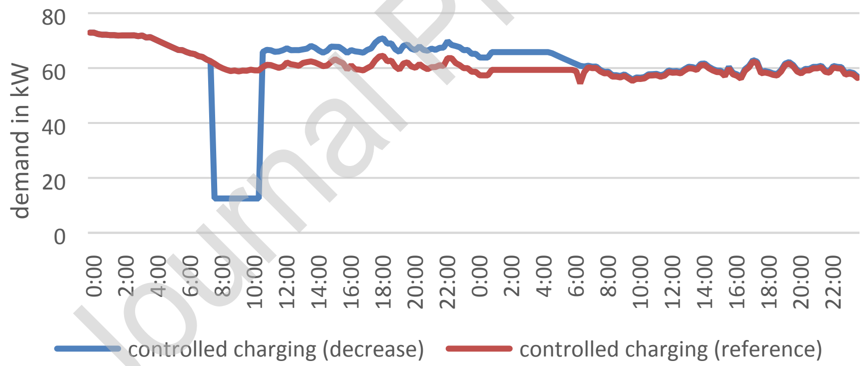


(c) $R = -50\ kW$, between 7:45 and 10:45 of the first day

Fig.8. Synergy with wind energy integration

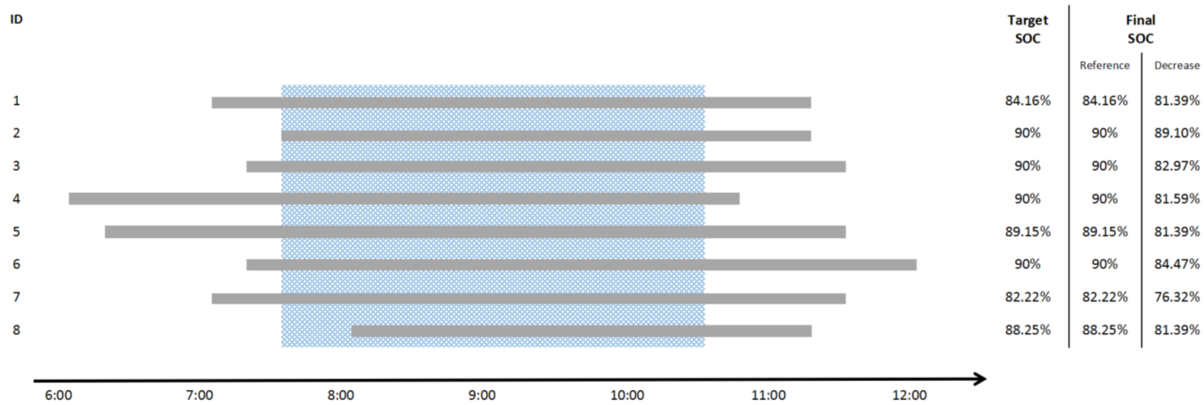


Fig. 9. Comparison of final SOC at departure, reference case of Fig. 8 and decrease case of Fig. 8(c)

Due to the possibility of uncompleted charging tasks, we further calculate the lowest R value for temporary decrease which can still complete all charging tasks. To achieve this, we adjust the original model ((1) - (18)) as follows.

Min: $D_i^I + \sum_\omega \sum_{t=i+1}^{t=W^i} \pi_\omega \times (|D_{t,\omega}^I| + |D_{t,\omega}^{II}|) - \mathrm{M} \times \overline{R}$ (1a)

$SOC_{m,t} \geq SOC_m^{target} \times (1 - AA_m)$ $\quad m \in EV^i, t = W^i$ (10a)

$SOC'_{s,t,\omega} \geq SOC_s^{target}$ $\quad t = W^i, s \geq i+1, \forall\omega$ (17a)

$D_{t,\omega} + \overline{R} = D_{i-1}^{ref}$ $\quad i \leq t \leq i+q, i \geq 2, \forall\omega$ (27)

Objective (1) is replaced by (1a). Parameter M is set to be a large positive number. Variable $\overline{R}$ is the amount for temporary decrease and can be either positive or negative by definition. To minimize the objective, $\overline{R}$ will try to be as large as possible.

Constraint (10) and (17) are replaced by (10a) and (17a) respectively. We remove $Gap_m$ and $Gap'_{s,\omega}$ from the constraints to guarantee that all charging tasks can be completed.

Constraint (25) is an additional constraint. Parameter $D_{i-1}^{ref}$ is the total charging demand in the last period in the reference case (shown in Fig. 8). With constraint (25), the new model will force the total charging demand to be lower than $D_{i-1}^{ref}$ by a certain amount $\overline{R}$ for a couple of periods. The new model includes objective (1a), constraints (2-9), (10a), (11-16), (17a), (18) and (27).

Fig. 10 shows the exemplary 2-day results of the lowest operating level (compared with the reference case) if we decrease the total charging demand temporarily for two or three hours. The initial charging curve from ***Application I*** serves as a reference case before control reserve is provided. From either one of the two lowest operating level curves, we can see that this lowest operating level is time-variant because EVs parking at night have longer parking times and greater load shifting potentials. When we compare the two curves, we find that this lowest operating level is higher for longer decrease durations.

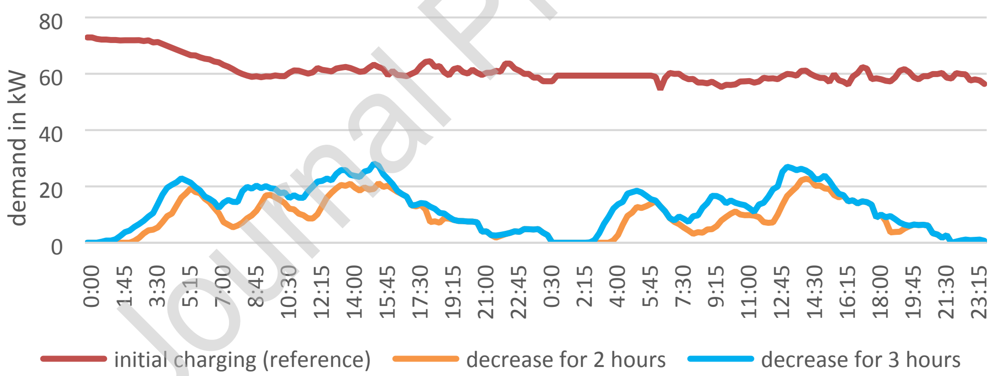


Fig. 10. Lowest operating level for temporary decrease

In Fig. 8(c), we have a decrease of 50 kW from 7:45 to 10:45 on the first day. While in Fig. 10, the $\overline{R}$ value for three hours at 7:45 of the first day is 47.99 kW, which means uncompleted charging will happen if the decrease value is greater than 47.99 kW and lasts for three hours. In order to justify the new model, we set R to be -47.99 kW from 7:45 to 10:45 and rerun the original model with constraint (24). We check if all EV charging tasks can be completed in this new decrease case. In Fig. 11, we compare the final SOC results of this new decrease case with the one in the reference case of Fig. 8. We illustrate the charging availabilities of the tasks with gray bars and the decrease periods with blue shades (from 7:45 to 10:45 of the 1st day).

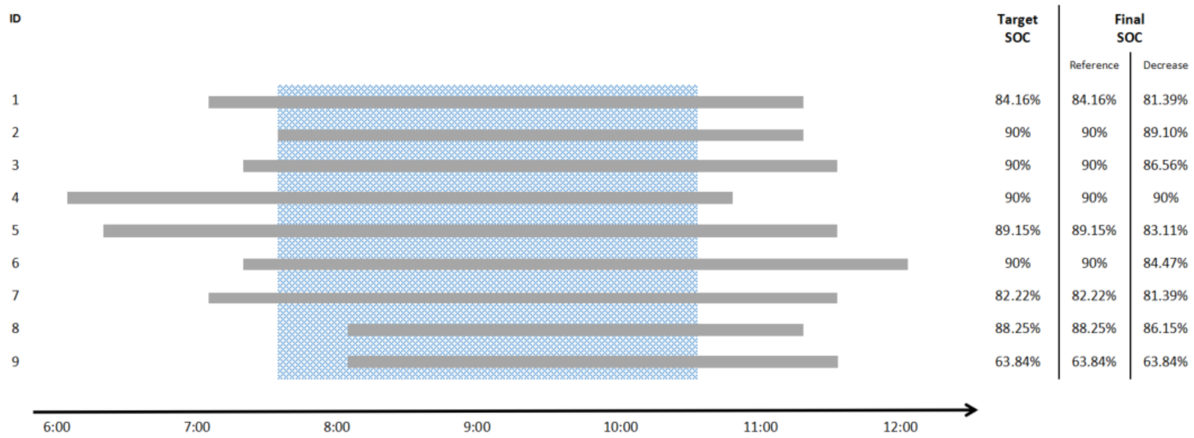


Fig. 11. Comparison of final SOC at departure, reference case of Fig. 8 and new decrease case ($R = -47.99\ kW$, between 7:45 and 10:45 of the 1st day)

In Fig. 11, the first eight tasks are the same as the ones in Fig. 9 and we see that seven tasks are still uncompleted (Tasks 1-3 and 5-8), which means the $\overline{R}$ value from the new model fails to guarantee that all charging tasks can be completed. This is because the new model can only guarantee that all EVs that are already connected at 7:45 can complete their charging tasks. Based on the EV patterns used, Task 8 is available from 8:15 to 11:30 and Task 9 from 8:15 to 11:45. These two EV arrive during the 3-hour period and have limited availabilities for load shifting, which takes up the charging demand scheduled for other EVs (Task 1-3 and 5-8). As a result, some EV charging tasks are uncompleted. Even though our model considers uncertainties of future EVs, the total charging demand is controlled at a low level in the first three hours of the decrease case so that the model does not schedule charging behaviors for future EVs within the decrease periods.

Despite the discussions above, the findings in Fig. 10 provide an upper bound for real-time charging demand decrease, which means uncompleted charging tasks will happen if the decrease level goes beyond $\overline{R}$. The findings may assist EVs in integrating renewable energy or bidding in control reserve markets. Fig. 10 can also serve as a quantification of EV load shifting potentials at different times of the day. Future work may focus on further improvements of the new model.

### 5.5 Future Work

As a premise to our proposed model, we assume that all EV users accept the proposed charging strategy and that none of them will leave earlier than at their guaranteed departure times. The simplifications above might not apply in reality and analyses of EV users' acceptance should be studied accordingly (Ensslem et al., 2013). Although we have taken into account the uncertainties of future EVs by either scenarios or valid assumptions, the EV driving profile with different maximum charging power in reality might be more difficult to consider than our simulation results, which might deteriorate the performance of the proposed model. Further exemplary results based on other EV database might be necessary. Since charging strategies may have a significant impact on the battery lifetime, additional concerns regarding the battery degradation could also be considered (X. Hu et al., 2016; Li et al., 2017). The applications of load flattening and peaking shaving can be further elaborated with constraints for grid bottleneck and transformer capacity limit and the synergy between EV charging and local renewable energy integration can also be further studied. As in Tan et al. (2016) and Zheng et al. (2019), the idea of V2G has been widely discussed in the current literature but is not yet included in our current model. The integration of V2G would increase model complexity and computational burden and would be an improvement of our work and the focus of future research.

## 6. Conclusion

This paper presents a two-stage SLP to address the EV charging scheduling problem in real time. We model the uncertainties in EV availability (arrival time and departure time) and SOC status upon arrival (initial SOC and target SOC). We consider the future EVs on an aggregated level to reduce computational burden. With this objective, the model can be easily applied for different optimization purposes.

Three potential applications are given. *Application I* flattens the total charging demand of an EV fleet throughout the day. A comparison between the controlled charging demand and an instant charging demand is presented. *Application II* is for peak shaving in coupling with household demand and manages to shift more charging demand to off-peak hours. *Application III* utilizes EVs for renewable energy integration where EV charging behaviors respond to the volatile output of renewable energy in real time, which can also serve as an example of participation in the control reserve market.

We show that future EVs may not complete their charging tasks when the down-regulation offer of total load is excessively provided and charging behaviors are greatly postponed. This is because we consider the uncertainties from future EVs but on an aggregated level. This aggregation decreases the computation complexity of the model and does not consider EVs which arrive in the near future with limited availabilities. Based on this, we further adjust the model and calculate the upper bound down-regulation offer at different times of the day and for different durations.

**Acknowledgements**

The work presented here is funded by Helmholtz Research School on Energy Scenarios.

**References**

Akhavan-Rezai, E., Shaaban, M.F., El-Saadany, E.F., Karray, F., 2018. New EMS to incorporate smart parking lots into demand response. IEEE Trans. Smart Grid. https://doi.org/10.1109/TSG.2016.2587901

Babrowski, S., Heinrichs, H., Jochem, P., Fichtner, W., 2014. Load shift potential of electric vehicles in Europe. J. Power Sources. https://doi.org/10.1016/j.jpowsour.2014.01.019

Baringo, L., Sánchez Amaro, R., 2017. A stochastic robust optimization approach for the bidding strategy of an electric vehicle aggregator. Electr. Power Syst. Res. https://doi.org/10.1016/j.epsr.2017.02.004

Brady, J., O'Mahony, M., 2016. Modelling charging profiles of electric vehicles based on real-world electric vehicle charging data. Sustain. Cities Soc. https://doi.org/10.1016/j.scs.2016.06.014

Ensslem, A., Jochem, P., Schäuble, J., Babrowski, S., Fichtner, W., 2013. User Acceptance of Electric Vehicles in the French-German Transnational Context: Results out of the french-german fleet test "cross-border mobility for electric vehicles" (CROME). Proc. 13th WCTR. https://doi.org/10.5445/IR/1000045139

Feng, Y., Ryan, S.M., 2013. Scenario construction and reduction applied to stochastic power generation expansion planning. Comput. Oper. Res. https://doi.org/10.1016/j.cor.2012.05.005

Fischer, D., Harbrecht, A., Surmann, A., McKenna, R., 2019. Electric vehicles' impacts on residential electric local profiles – A stochastic modelling approach considering socio-economic, behavioural and spatial factors. Appl. Energy. https://doi.org/10.1016/j.apenergy.2018.10.010

Goonewardena, M., Le, L.B., 2012. Charging of electric vehicles utilizing random wind: A stochastic optimization approach, in: 2012 IEEE Globecom Workshops, GC Wkshps 2012. https://doi.org/10.1109/GLOCOMW.2012.6477811

Guo, L., Erliksson, K.F., Low, S.H., 2018. Optimal online adaptive electric vehicle charging, in: IEEE Power and Energy Society General Meeting. https://doi.org/10.1109/PESGM.2017.8274166

He, Y., Venkatesh, B., Guan, L., 2012. Optimal scheduling for charging and discharging of electric vehicles. IEEE Trans. Smart Grid. https://doi.org/10.1109/TSG.2011.2173507

Heitsch, H., Römisch, W., 2003. Scenario reduction algorithms in stochastic programming. Comput. Optim. Appl. https://doi.org/10.1023/A:1021805924152

Heydarian-Forushani, E., Golshan, M.E.H., Shafie-khah, M., 2016. Flexible interaction of plug-in electric vehicle parking lots for efficient wind integration. Appl. Energy. https://doi.org/10.1016/j.apenergy.2016.06.145

Hu, J., Morais, H., Sousa, T., Lind, M., 2016. Electric vehicle fleet management in smart grids: A review of services, optimization and control aspects. Renew. Sustain. Energy Rev. https://doi.org/10.1016/j.rser.2015.12.014

Hu, X., Li, S.E., Yang, Y., 2016. Advanced Machine Learning Approach for Lithium-Ion Battery State Estimation in Electric Vehicles. IEEE Trans. Transp. Electrif. https://doi.org/10.1109/TTE.2015.2512237

Hu, Z., Zhan, K., Zhang, H., Song, Y., 2016. Pricing mechanisms design for guiding electric vehicle charging to fill load valley. Appl. Energy 178, 155–163. https://doi.org/10.1016/j.apenergy.2016.06.025

Iversen, E.B., Moller, J.K., Morales, J.M., Madsen, H., 2017. Inhomogeneous Markov Models for Describing Driving Patterns. IEEE Trans. Smart Grid. https://doi.org/10.1109/TSG.2016.2520661

Iversen, E.B., Morales, J.M., Madsen, H., 2014. Optimal charging of an electric vehicle using a Markov decision process. Appl. Energy. https://doi.org/10.1016/j.apenergy.2014.02.003

iZEUS, 2012. KIT-Forschungsprojekt iZEUS - Startseite [WWW Document]. URL http://www.izeus.kit.edu (accessed 11.1.19).

Jochem, P., Landes, P., Reuter-Oppermann, M., Fichtner, W., 2016. Workload patterns of fast charging stations along the German Autobahn. Proc. EVS29 Symp. Montréal, Québec, CDN, June 19-22, 2016.

Ju, L., Li, H., Zhao, J., Chen, K., Tan, Q., Tan, Z., 2016. Multi-objective stochastic scheduling optimization model for connecting a virtual power plant to wind-photovoltaic-electric vehicles considering uncertainties and demand response. Energy Convers. Manag. https://doi.org/10.1016/j.enconman.2016.09.072

Kaschub, T., Heinrichs, H., Jochem, P., Fichtner, W., 2013. Modeling Load Shifting Potentials of Electric Vehicles, in: 13th IAEE European Conference. Düsseldorf, Germany.

Le Goff Latimier, R., Multon, B., Ben Ahmed, H., Baraer, F., Acquitter, M., 2015. Stochastic optimization of an Electric Vehicle Fleet Charging with Uncertain Photovoltaic Production, in: 2015 International Conference on Renewable Energy Research and Applications, ICRERA 2015. https://doi.org/10.1109/ICRERA.2015.7418505

Lee, Z.J., Chang, D., Jin, C., Lee, G.S., Lee, R., Lee, T., Low, S.H., 2019. Large-scale adaptive electric vehicle charging, in: 2018 IEEE Global Conference on Signal and Information Processing, GlobalSIP 2018 - Proceedings. https://doi.org/10.1109/GlobalSIP.2018.8646472

Li, Z., Huang, J., Liaw, B.Y., Zhang, J., 2017. On state-of-charge determination for lithium-ion batteries. J. Power Sources. https://doi.org/10.1016/j.jpowsour.2017.03.001

Liu, J., 2012. Electric vehicle charging infrastructure assignment and power grid impacts assessment in Beijing. Energy Policy. https://doi.org/10.1016/j.enpol.2012.08.074

Lu, X., Zhou, K., Yang, S., Liu, H., 2018. Multi-objective optimal load dispatch of microgrid with stochastic access of electric vehicles. J. Clean. Prod. https://doi.org/10.1016/j.jclepro.2018.05.190

Lunz, B., Yan, Z., Gerschler, J.B., Sauer, D.U., 2012. Influence of plug-in hybrid electric vehicle charging strategies on charging and battery degradation costs. Energy Policy. https://doi.org/10.1016/j.enpol.2012.04.017

Mehrjerdi, H., Rakhshani, E., 2019. Vehicle-to-grid technology for cost reduction and uncertainty management integrated with solar power. J. Clean. Prod. https://doi.org/10.1016/j.jclepro.2019.05.023

Morais, H., Sousa, T., Vale, Z., Faria, P., 2014. Evaluation of the electric vehicle impact in the power demand curve in a smart grid environment. Energy Convers. Manag. https://doi.org/10.1016/j.enconman.2014.03.032

Perez, H.E., Hu, X., Dey, S., Moura, S.J., 2017. Optimal Charging of Li-Ion Batteries with Coupled Electro-Thermal-Aging Dynamics. IEEE Trans. Veh. Technol. https://doi.org/10.1109/TVT.2017.2676044

Ramchurn, B.S.D., 2012. Putting the ‘ Smarts ’ into the Smart Grid : a Grand challenge for artificial intelligence. Commun. ACM. https://doi.org/10.1145/2133806.2133825

Richardson, P., Flynn, D., Keane, A., 2012. Local versus centralized charging strategies for electric vehicles in low voltage distribution systems. IEEE Trans. Smart Grid. https://doi.org/10.1109/TSG.2012.2185523

Sabillon Antunez, C., Franco, J.F., Rider, M.J., Romero, R., 2016. A New Methodology for the Optimal Charging Coordination of Electric Vehicles Considering Vehicle-to-Grid Technology. IEEE Trans. Sustain. Energy 7, 596–607. https://doi.org/10.1109/TSTE.2015.2505502

Sarker, M.R., Dvorkin, Y., Ortega-Vazquez, M.A., 2016. Optimal participation of an electric vehicle aggregator in day-ahead energy and reserve markets. IEEE Trans. Power Syst. https://doi.org/10.1109/TPWRS.2015.2496551

Schäuble, J., Jochem, P., Fichtner, W., 2016. Cross-border Mobility for Electric Vehicles: Selected results from one of the first cross-border field tests in Europe, Cross-border Mobility for Electric Vehicles. https://doi.org/10.5445/KSP/1000052445

Schäuble, J., Kaschub, T., Ensslen, A., Jochem, P., Fichtner, W., 2017. Generating electric vehicle load profiles from empirical data of three EV fleets in Southwest Germany. J. Clean. Prod. https://doi.org/10.1016/j.jclepro.2017.02.150

Schermeyer, H., Vergara, C., Fichtner, W., 2018. Renewable energy curtailment: A case study on today’s and tomorrow’s congestion management. Energy Policy. https://doi.org/10.1016/j.enpol.2017.10.037

Schill, W.P., Gerbaulet, C., 2015. Power system impacts of electric vehicles in Germany: Charging with coal or renewables? Appl. Energy. https://doi.org/10.1016/j.apenergy.2015.07.012

Schuller, A., Flath, C.M., Gottwalt, S., 2015. Quantifying load flexibility of electric vehicles for renewable energy integration. Appl. Energy. https://doi.org/10.1016/j.apenergy.2015.04.004

Seddig, K., Jochem, P., Fichtner, W., 2019. Two-stage stochastic optimization for cost-minimal charging of electric vehicles at public charging stations with photovoltaics. Appl. Energy 769–781. https://doi.org/10.1016/j.apenergy.2019.03.036

Seddig, K., Jochem, P., Fichtner, W., 2017. Integrating renewable energy sources by electric vehicle fleets under uncertainty. Energy. https://doi.org/10.1016/j.energy.2017.11.140

Sundström, O., Binding, C., 2012. Flexible charging optimization for electric vehicles considering distribution grid constraints. IEEE Trans. Smart Grid. https://doi.org/10.1109/TSG.2011.2168431

Sundström, O., Binding, C., 2011. Charging service elements for an electric vehicle charging service provider, in: IEEE Power and Energy Society General Meeting. https://doi.org/10.1109/PES.2011.6038982

Taljegard, M., Göransson, L., Odenberger, M., Johnsson, F., 2019. Impacts of electric vehicles on the electricity generation portfolio – A Scandinavian-German case study. Appl. Energy. https://doi.org/10.1016/j.apenergy.2018.10.133

Tan, K.M., Ramachandaramurthy, V.K., Yong, J.Y., 2016. Integration of electric vehicles in smart grid: A review on vehicle to grid technologies and optimization techniques. Renew. Sustain. Energy Rev. https://doi.org/10.1016/j.rser.2015.09.012

Wang, Y., 2010. Scenario reduction heuristics for a rolling stochastic programming simulation of bulk energy flows with uncertain fuel costs. Iowa State University, Digital Repository, Ames. https://doi.org/10.31274/etd-180810-1878

Wellers, M., Martinez, C.M., Gao, B., Velenis, E., Hu, X., Cao, D., 2016. Energy Management in Plug-in Hybrid Electric Vehicles: Recent Progress and a Connected Vehicles Perspective. IEEE Trans. Veh. Technol. https://doi.org/10.1109/tvt.2016.2582721

Widén, J., Nilsson, A.M., Wäckelgård, E., 2009. A combined Markov-chain and bottom-up approach to modelling of domestic lighting demand. Energy Build. https://doi.org/10.1016/j.enbuild.2009.05.002

Wu, F., Sioshansi, R., 2017. A two-stage stochastic optimization model for scheduling electric vehicle charging loads to relieve distribution-system constraints. Transp. Res. Part B Methodol. https://doi.org/10.1016/j.trb.2017.05.002

Wu, X., Hu, X., Moura, S., Yin, X., Pickert, V., 2016. Stochastic control of smart home energy management with plug-in electric vehicle battery energy storage and photovoltaic array. J. Power Sources. https://doi.org/10.1016/j.jpowsour.2016.09.157

Yang, Z., Li, K., Foley, A., 2015. Computational scheduling methods for integrating plug-in electric vehicles with power systems: A review. Renew. Sustain. Energy Rev. https://doi.org/10.1016/j.rser.2015.06.007

Zhang, H., Moura, S.J., Hu, Z., Qi, W., Song, Y., 2018. Joint PEV Charging Network and Distributed PV Generation Planning Based on Accelerated Generalized Benders Decomposition. IEEE Trans. Transp. Electrif. https://doi.org/10.1109/TTE.2018.2847244

Zhang, T., Chen, W., Han, Z., Cao, Z., 2014. Charging scheduling of electric vehicles with local renewable energy under uncertain electric vehicle arrival and grid power price. IEEE Trans. Veh.

Technol. https://doi.org/10.1109/TVT.2013.2295591

Zheng, Y., Niu, S., Shang, Y., Shao, Z., Jian, L., 2019. Integrating plug-in electric vehicles into power grids: A comprehensive review on power interaction mode, scheduling methodology and mathematical foundation. Renew. Sustain. Energy Rev. https://doi.org/10.1016/j.rser.2019.05.059

Authors’ individual contributions

**Zongfei Wang**: Conceptualization, Methodology, Software, Formal analysis, Investigation, Data Curation, Writing - Original Draft, Visualization

**Patrick Jochem**: Validation, Resources, Investigation, Writing - Review & Editing, Supervision, Funding acquisition

**Wolf Fichtner**: Validation, Resources, Writing - Review & Editing, Supervision, Funding acquisition

**Declaration of interests**

☐ The authors declare that they have no known competing financial interests or personal relationships that could have appeared to influence the work reported in this paper.

☐The authors declare the following financial interests/personal relationships which may be considered as potential competing interests:

Ms. Zongfei Wang
PD Dr. Patrick Jochem
Prof. Dr. Wolf Fichtner